A Microwave Snow Emissivity Model

Fuzhong Weng
Joint Center for Satellite Data Assimilation
NOAA/NESDIS/Office of Research and Applications, Camp Springs, Maryland
and
Banghua Yan
Decision Systems Technologies Inc., Rockville, Maryland

Abstract

This paper presents a new microwave snow emissivity model which is empirically derived from satellite retrievals and ground-based measurements. This model produces a variety of snow emissivity spectra at microwave frequencies according to snow types. As part of this model, an algorithm is also developed to classify snow type using the Advanced Microwave Sounding Unit (AMSU) measurements at 23.8, 31.4, 50.3, 89 and 150 GHz. It is shown that the global snow emissivity simulated with this model agrees with that retrieved from satellite measurements.

1. Introduction

Information on land surface emissivity is important for both satellite data assimilation schemes and retrievals of atmospheric parameters from satellite measurements. Recently, a model was developed to simulate the emissivity over various land conditions including snow [Weng et al., 2001] and has been operationally used in the National Centers for Environmental Prediction (NCEP) global forecast system data assimilation system (GDAS). It is found that the discrepancies between simulated and observed brightness temperatures are significant in the polar areas where snow has been probably metamorphosed and vertically stratified [Weng et al., 2001].

Microwave emissivity at the frequencies ranging from 20 to 150 GHz over land can be directly retrieved from satellite measurements [Jones and Vonder Haar, 1997; Prigent et al., 1997; Yan and Weng, 2002]. Statistical information on emissivity such as mean and standard deviation was also generated at the Special Sensor Microwave Imager (SSM/I) frequencies [Yan and Weng, 2002]. It was shown that snow emissivity strongly varies with season and surface types. In this study, we use both satellite retrievals and the ground-based estimations from Mätzler [1994] to derive a new emissivity model.

2. The Nature of Problems

The brightness temperature, T_B, emanating from a scattering-free atmosphere is related to surface emissivity, ε, through

$$T_B = \varepsilon T_s \tau + T_u + (1-\varepsilon) T_d \tau \qquad (1)$$

where T_s is the surface temperature, T_u and T_d are the brightness temperatures associated with upwelling and downwelling radiation, respectively, and τ is the atmospheric transmittance. In the satellite data assimilation scheme, we need to calculate the brightness temperatures at various frequencies with a surface emissivity model. An error in emissivity is directly translated into the error in brightness temperature, viz.

$$\Delta T_B = \tau (T_s - T_d) \Delta\varepsilon \, . \qquad (2)$$

Table 1 displays the errors of brightness temperatures at the Advanced Microwave Sounding Unit (AMSU) frequencies for $\Delta\varepsilon$ of 0.04. Obviously, at a window channel where τ is relatively larger and T_d is smaller, the emissivity uncertainty has a much larger impact on the brightness temperature.

For example, at 150 GHz, ΔT_B is about 7.0 °K when total precipitable water, *TPW*, is 2 mm, T_s is 230 °K and surface pressure, P_s, is 1000 mb. For P_s of 600 mb, ΔT_B increases to about 8.0 °K. At the sounding channels near 50-60 GHz oxygen absorption band, ΔT_B decreases as the frequency approaches to the center of the absorption band. At 52.8 GHz, ΔT_B increases from 0.2 °K to 2.3 °K as P_s decreases from 1000 mb to 600 mb.

Table 1. Errors of brightness temperatures (ΔT_B) in relation to the errors of surface emissivity.

Freq (GHz)	Ts = 230 K and TPW = 0.5 mm						Ts = 230 K and TPW = 2.0 mm					
	Ps = 600 (mb)			Ps = 1000 (mb)			Ps = 600 (mb)			Ps = 1000 (mb)		
	T_d(K)	τ	ΔT_B(K)	T_d(K)	τ	ΔT_B(K)	T_d(K))	τ	ΔT_B(K)	T_d(K)	τ	ΔT_B(K)
50.3	49.30	0.774	5.593	112.5	0.487	2.289	49.8	0.771	5.559	113.6	0.483	2.247
52.8	111.2	0.492	2.337	188.6	0.153	0.253	111.6	0.490	2.322	189.0	0.151	0.248
150	4.4	0.980	8,844	12.5	0.944	8.209	11.4	0.949	8.295	32.3	0.856	6.771
183.3±7	16.6	0.925	7.893	43.5	0.807	6.018	57.9	0.739	5.087	127.8	0.435	1.786
183.3±3	55.3	0.750	5.242	104.1	0.538	2.709	151.6	0.320	1.005	208.1	0.086	0.076
183.3±1	134.6	0.392	1.496	160.1	0.288	0.806	219.8	0.024	0.010	227.2	0.007	0.001

At the sounding channels near the 183.3 GHz water vapor absorption band, ΔT_B strongly varies with *TPW*, P_s and frequency. At 183.3±7 GHz which is the furthest from the band center, ΔT_B increases from 1.8 °K to 6.0 °K as *TPW* decreases from 2.0 mm to 0.5 mm for P_s of 1000 mb. For P_s of 600 mb, ΔT_B is up to 7.9 °K. At 183.3±1 GHz, the impact of surface emissivity on the brightness temperature is the smallest (~ 0.01 °K) for a *TPW* of 2.0 mm. However, for a drier atmosphere, the impact is significantly higher, especially over a region where the surface pressure is lower. For example, ΔT_B at 183.3±1 GHz increases from 0.8°K to 1.5 °K as P_s decreases from 1000 mb to 600 mb for a *TPW* of 0.5 mm. This implies that the uncertainty in surface emissivity over a high-elevation terrain and under a moisture deficient atmosphere will significantly increase the uncertainty in simulating the brightness temperatures at microwave sounding channels.

3. Microwave Snow Emissivity Spectra

3.1 Microwave Emissivity Spectra

In this study, the emissivity is retrieved from satellite and ground-based measurements at various frequencies and is further used to produce the entire spectra over various snow conditions. At microwave frequencies between 4.9 and 94 GHz, eleven snow emissivity spectra over Switzerland were reported by Mätzler (1994). While Mätzler's studies provide the unique information of snow emissivity at lower frequency, there are some deficiencies in the two following aspects: 1) There is no emissivity information at frequencies above 94 GHz, and 2) there are some obvious gaps in two neighborhood emissivity spectra. Thus, satellite retrieved emissivity offers some information complementary to the ground-based estimates.

Using the AMSU measurements at five window channels collocated with radiosonde temperature and water vapor profiles, we calculate snow emissivity between 23.8 and 150 GHz under clear-sky conditions. It is found that several emissivity spectra are frequently observed from these AMSU measurements yet they were not included in Mätzler's data sets. Therefore, these two data sets have been combined to obtain the emissivity spectra at the frequencies ranging from 4.9 to 150 GHz. Since the AMSU measures weighted radiances from vertical and horizontal polarization, Mätzler's data sets are also combined using

$$\varepsilon = \cos^2(\theta)\varepsilon_v + \sin^2(\theta)\varepsilon_h \qquad (3)$$

where θ is the local zenith angle, ε_v and ε_h are the emissivity at vertical and horizontal polarization, respectively. Figure 1 displays sixteen emissivity spectra vs. frequency at the local zenith angle of 50 degree. At 4.9 GHz, the emissivity is least dependent on snow types because of the weakest scattering effects from snow. The largest variability in the emissivity spectra occurs at higher frequencies due primarily to the variability of volumetric scattering within snow.

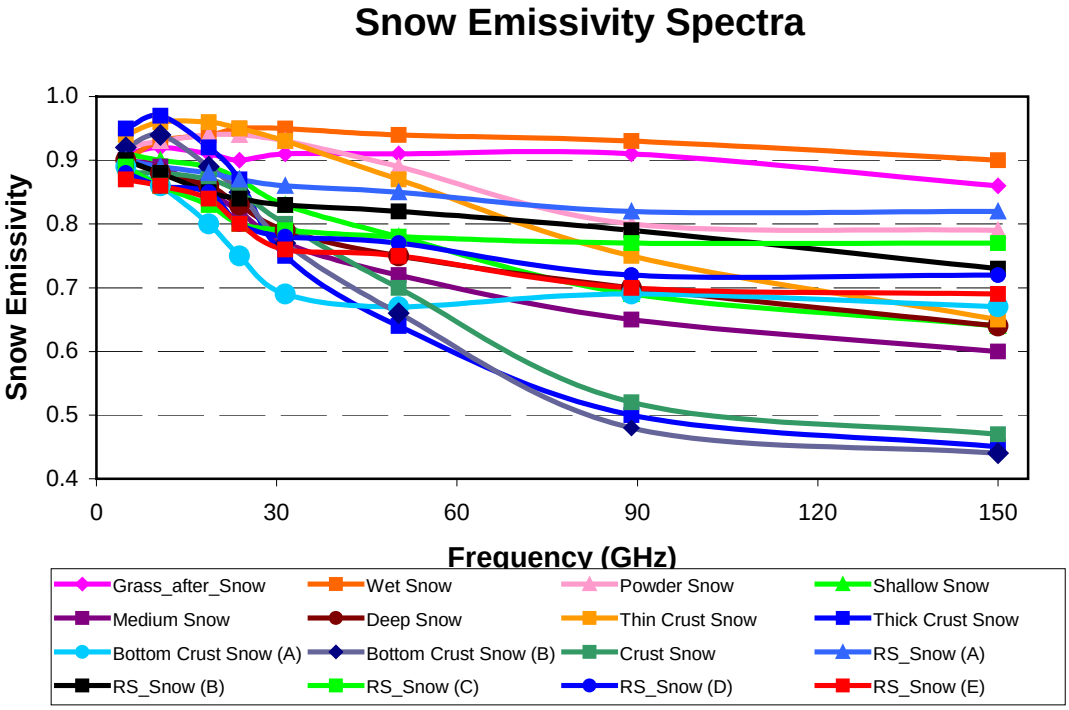

Figure 1. Microwave emissivity as a function of frequency across the range between 4.9 and 150 GHz for sixteen snow surfaces. The type indicated by "RS", radiometric snow, implies a distinct emissivity spectrum but can't be directly associated with a physical snow type. **1.** Wet snow: at least a wet surface layer; **2.** Grass_after_Snow: short grass on a flat ground after snow melts; **3.** RS (A): radiometric type; **4.** Power snow: 24 – 37 cm deep at temperature ranging from –3 to –13 ^{o}C; **5 – 7.** RS (B~D): radiometric types; **8**. Thin crust: wet snow covered by refrozen crust whose thickness is 1-3 cm; **9.** RS: radiometric type; **10.** Bottom crust (A): snow metamorphosed to a thick, hard crust (~ 40 cm) formed at the bottom of the new winter snow; **11.** Shallow: dry winter snow having water equivalent (WE) of 4 – 10 cm and having not undergone melting and metamorphism; **12.** Deep: winter snow having a WE of 25 – 63 cm; **13.** Crust: a layer of refrozen snow (~10 cm) on the top of a wet thin snow (~ 3 cm) with unfrozen ground; **14.** Medium depth: winter snow having a WE of 10 – 25 cm; **15.** Bottom crust (B): aged and refrozen snow on frozen ground (6 to 15 cm), **16.** Thick crust: wet snow covered by a refrozen layer of 4 – 30 cm.

3.2 Identification of Snow Type

To use the emissivity information in Fig. 1, we must first identify the snow type. Using the AMSU five window channel measurements, we develop several discriminators (DI_0 ~DI_5). These

discriminators are used to estimate the intensities of emissivity differences between five pairs of frequencies (e.g. 23.8/31.4, 31.4/ 89.0, 31.4/150.0, 50.3/150.0, 89.0/150.0),

$$DI_0 = a_0 + a_1 T_{B1} + a_2 T_{B1}^2 + a_3 T_{B2} + a_4 T_{B2}^2 + a_5 T_{B3} + a_6 T_{B3}^2, \quad (4a)$$

and

$$DI_j = a_0 + a_1 T_{B2} + \sum_{i=1}^{5} a_{(i+1)} DT_{B1} \ (j = 1 \sim 5), \quad (4b)$$

where

$$DT_{B1} = T_{B1} - T_{B2}, \quad (5a)$$
$$DT_{B2} = T_{B2} - T_{B4}, \quad (5b)$$
$$DT_{B3} = T_{B2} - T_{B5}, \quad (5c)$$
$$DT_{B4} = T_{B3} - T_{B5}, \quad (5d)$$
$$DT_{B5} = T_{B4} - T_{B5}. \quad (5d)$$

and T_{B1}, T_{B2}, T_{B3}, T_{B4}, T_{B5} are brightness temperature at 23.8, 31.4, 50.3, 89, 150 GHz, respectively. Here, coefficients $a_0 \sim a_6$ are listed in Table 2.

Table 2. Coefficients used to compute various discriminators ($DI_0 \sim DI_5$, LI, HI, $DS_1 \sim DS_3$) in snow type classification algorithm.

Indices	**Coefficients**						
	a_0	a_1	a_2	a_3	a_4	a_5	a_6
DI_0	1.72E+00	6.940E-03	2.02E-05	1.22E-02	1.23E-05	2.63E-02	4.88E-05
DI_1	2.67E-02	-1.23E-04	4.39E-03	-2.80E-03	2.92E-03	-8.46E-05	-2.84E-03
DI_2	-5.69E-02	2.07E-04	7.38E-04	1.38E-03	2.45E-03	1.20E-03	-3.46E-03
DI_3	-2.86E-01	1.21E-03	9.00E-04	7.10E-03	-4.21E-03	2.51E-03	6.96E-03
DI_4	-2.34E-01	1.02E-03	-4.02E-03	1.35E-02	-1.18E-02	2.31E-03	1.51E-02
DI_5	-2.26E-01	9.99E-04	1.62E-04	4.01E-03	-5.19E-03	1.31E-03	8.96E-03

Two indices, LI and HI, are also defined to estimate the intensity of surface emission at 31.4 and 150.0 GHz, respectively, viz.

$$LI = DI_0, \quad (6a)$$

$$HI = DI_0 - DI_3. \quad (6b)$$

Three additional indices, DS_1, DS_2 and DS_3 are defined as follows:

$$DS_1 = \sum_{i=1}^{2} DI_i \ , \quad (7a)$$

$$DS_2 = \sum_{i=4}^{5} DI_i \ , \quad (7b)$$

$$DS_3 = \sum_{i=1}^{5} DI_i \ ,. \quad (7c)$$

to describe the emissivity variation within a broader frequency range. For example, smaller DS_1 and DS_2 indicate less variation of snow emissivity within lower and higher frequency range, which are characteristics of fresh or wet or shallow snow. On the other hand, larger DS_1 and DS_2 imply a rapid decrease of emissivity within lower and higher frequency range, which are typical of aged or refrozen or deep snows. In general, higher LI and HI with lower DS_1, DS_2 and DS_3 imply fresh and

shallow snow, whereas a higher LI but a lower HI with higher DS_1, DS_2 and DS_3 identify a deep wet snow covered by a thick layer of refrozen snow (e.g. crust snow). For each snow type, we develop various thresholds for all indices (see Table 3). The brightness temperature at 150 GHz (T_{B5}) itself also helps a further classification of some snow types.

Table 3. Thresholds of various discriminators developed for snow type classification.

Snow Type	**Thresholds**					
	LI	HI	DS_1	DS_2	DS_3	T_{B5}
1	≥0.83	≥0.86	-	≤0.01	≤0.01	≥200.
	≥0.87	≥0.85	-	≤0.06	≤0.10	≥200.
	≥0.87	≥0.83	≤ -0.02	≤0.12	≤0.16	≥204.
	≥0.90	≥0.89	-	-	-	-
	≥0.92	≥0.85	-	-	-	-
2	≥0.84	≥0.83	-	≤0.08	≤0.10	≥195.
	≥0.85	≥0.85	-	≤0.10	-	≥190.
	≥0.86	≥0.81	-	≤0.12	-	≥200.
	≥0.86	≥0.81	≤ 0.00	≤0.12	-	≥189.
	≥0.90	≥0.81	-	-	-	≥195.
3	≥0.80	≥0.76	-	≤0.05	-	≥185.
	≥0.82	≥0.78	-	-	≤0.25	≥180.
	≥0.90	≥0.76	-	-	-	≥180.
4	≥0.89	≥0.73	-	≤0.20	-	-
	≥0.89	≥0.75	-	-	-	-
	≥0.93	≥0.72	-	-	-	-
5	≥0.81	≥0.70	-	≤0.20	-	≥160.
	≥0.83 ≤0.88	≥0.70 ≤0.78	-	-	-	≥160.
6	≥0.75	≥0.76	-	≤0.08	-	≥172.
	≥0.77	≥0.72	-	≤0.12	≤0.15	≥175.
	≥0.78	≥0.74	-	-	≤0.20	≥172.
	≥0.80	≥0.77	-	-	-	≥170.
	≥0.82	-	-	≤0.15	≤0.22	≥170.
	≥0.82	≥0.73	-	-	-	≥170.
7	≥0.75	≥0.70	-	≤0.15	≤0.25	≥167.
	≥0.77	≥0.76	-	-	-	-
	≥0.80	≥0.72	-	-	≤0.30	-
	≥0.77	≥0.73	-	-	≤0.25	-
	≥0.81	≥0.71	-	-	-	-
	≥0.82	≥0.69	-	-	-	-
8	≥0.88	≥0.58	-	-	-	-
9	≥0.73	≥0.67	-	-	-	-
10	≤0.83	≥0.66	-	-	-	-
11	≥0.82	≥0.61	-	-	-	-
12	≥0.77	≥0.58	-	-	-	-
13	≥0.77	≤0.52	-	-	-	-
14	≥0.74	≥0.55	-	-	-	-
15	≥0.74	-	-	-	-	-
16	-	-	-	-	-	-

Figure 2 displays the global snow types classified from NOAA-15 AMSU measurements on February 3, 2002. These snow types are best defined in a radiometric sense due to their distinct emissivity spectra. The snow types having smaller numbers are newly formed (shallow and powder), whereas those with larger numbers indicate aged snow (deep crust). In Northern Greenland and deep Antarctic regions, snow types are higher and probably deep crust. Also, the snow occurring over the western parts of North America and the northern parts of central Europe is newly formed and wet.

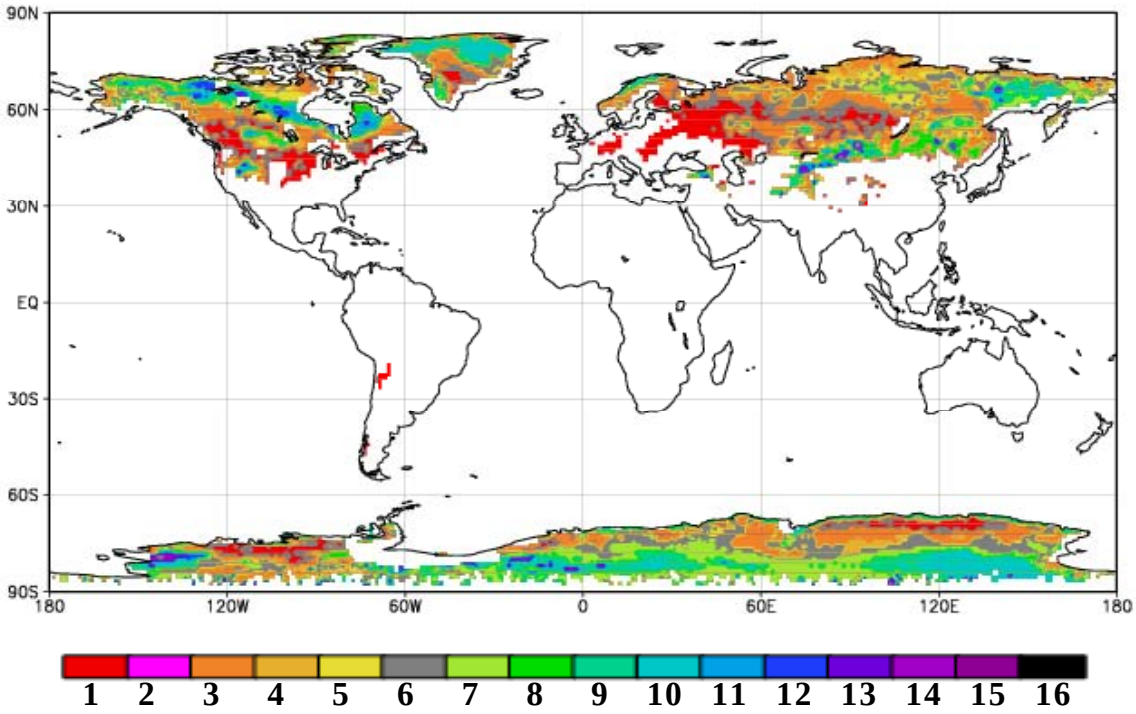

Figure 2. Global distribution of radiometric snow types derived from the AMSU.

4. Simulations of Global Snow Emissivity

Figures 3a and 3b display the emissivity maps at 31.4 GHz and 150 GHz simulated using the emissivity data in Fig. 1 and snow types in Fig. 2. The emissivity at 31.4 GHz is usually larger than 0.9 at mid- to high latitudes. Note that the emissivity at 31.4 GHz is less sensitive to snow type, compared to that at 150 GHz. Also, the emissivity at 150 GHz is lower for higher values of snow types (aged snow). For a snow type of 12 or greater (see Antarctic near 60^{o}W and Northern Alaska), the emissivity at 150 GHz could be as low as 0.6. The larger variability at 150 GHz is due primarily to an increasing volumetric scattering at high frequencies within snow.

Global snow emissivity simulated at a frequency range 5 – 150 GHz agrees well with that retrieved from the AMSU measurements. Figures 3c and 3d display the retrieved snow emissivity at 31.4 and 150 GHz, respectively. The retrievals are calculated using Eq. (1) with GDAS atmospheric temperature and water vapor profiles, and surface temperature. Since all optical parameters in Eq. (1) are computed without taking into account clouds, the emissivity may be overestimated over the areas where clouds and precipitation are present. (Note our analysis shows $\partial\varepsilon/\partial L > 0$, where L is the cloud liquid water path). For example, over the northern central Europe near the Caspian and Black Seas, the retrieved emissivity at 150 GHz is much higher than simulation due to clouds (cloud

image not shown here). Using the AMSU retrieved emissivity under cloud-free conditions, we found the errors of our snow emissivity model are generally less than 4 – 5%, with the smallest ones at higher frequencies (2 –3 %).

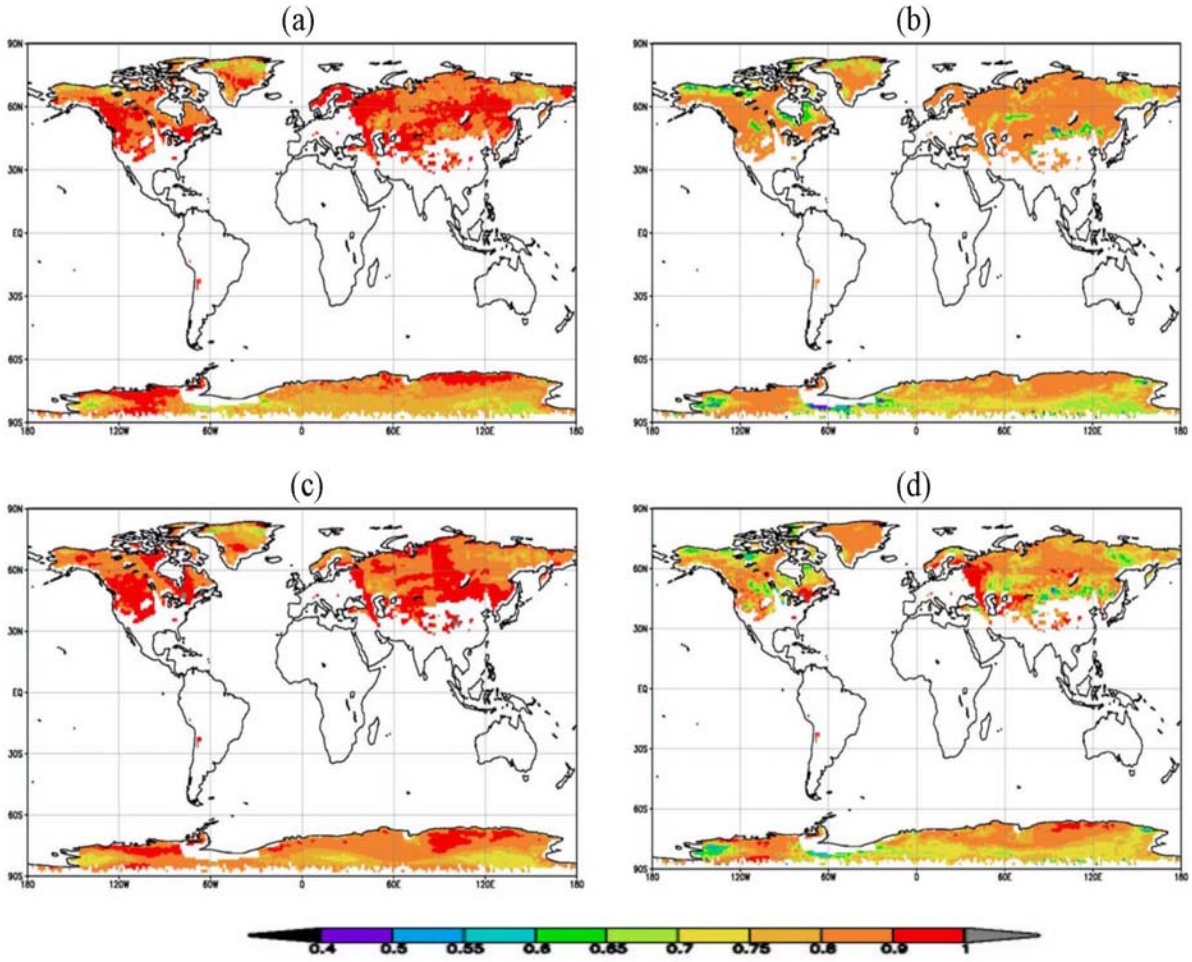

Figure 3. Global distributions of snow emissivity simulated from the model at (a) 31.4 GHz and (b) 150 GHz, compared with AMSU retrievals (c) and (d).

5. A Summary

A new snow emissivity model is developed using the retrievals from satellite and ground-based microwave measurements. The emissivity spectra are classified as sixteen types. An algorithm was developed to identify the snow through a set of discriminators that are defined with five AMSU window channel measurements. Global emissivity maps simulated with this newly developed model exhibit a reasonable distribution, and the errors of simulations are significantly reduced, compared with our earlier developed model.

Acknowledgements: This research is supported by Joint Center for Satellite Data Assimilation directed research program funds.

References

Jones, A. S. and T. H. Vonder Haar, 1997: Retrieval of microwave surface emittance over land using coincident microwave and infrared satellite measurements, *J. Geophys. Res*.,**102**, 13,609-13,626.

Mätzler, C., 1994: Passive microwave signatures of landscapes in winter, *Meteor. Atmos. Phys.*, **54**, 241-260.

Prigent, C., W. B. Rossow and E. Matthews, 1997: Microwave land surface emissvities estimated from SSM/I observations, *J. Geophys. Res*., **102**, 867-890.

Weng, F., B. Yan, and N. C. Grody, 2001: A microwave land emissivity model, *Geophys. Res.,* **106**, 20,115-20,123.

Yan, B. and F. Weng, 2002: A ten-year (1993-2002) time-series of microwave land emissivity, SPIE Third International Asia-Pacific Symposium, Hangzhou, China.

Proceedings of the Thirteenth International TOVS Study Conference

INTERNATIONAL ATOVS WORKING GROUP

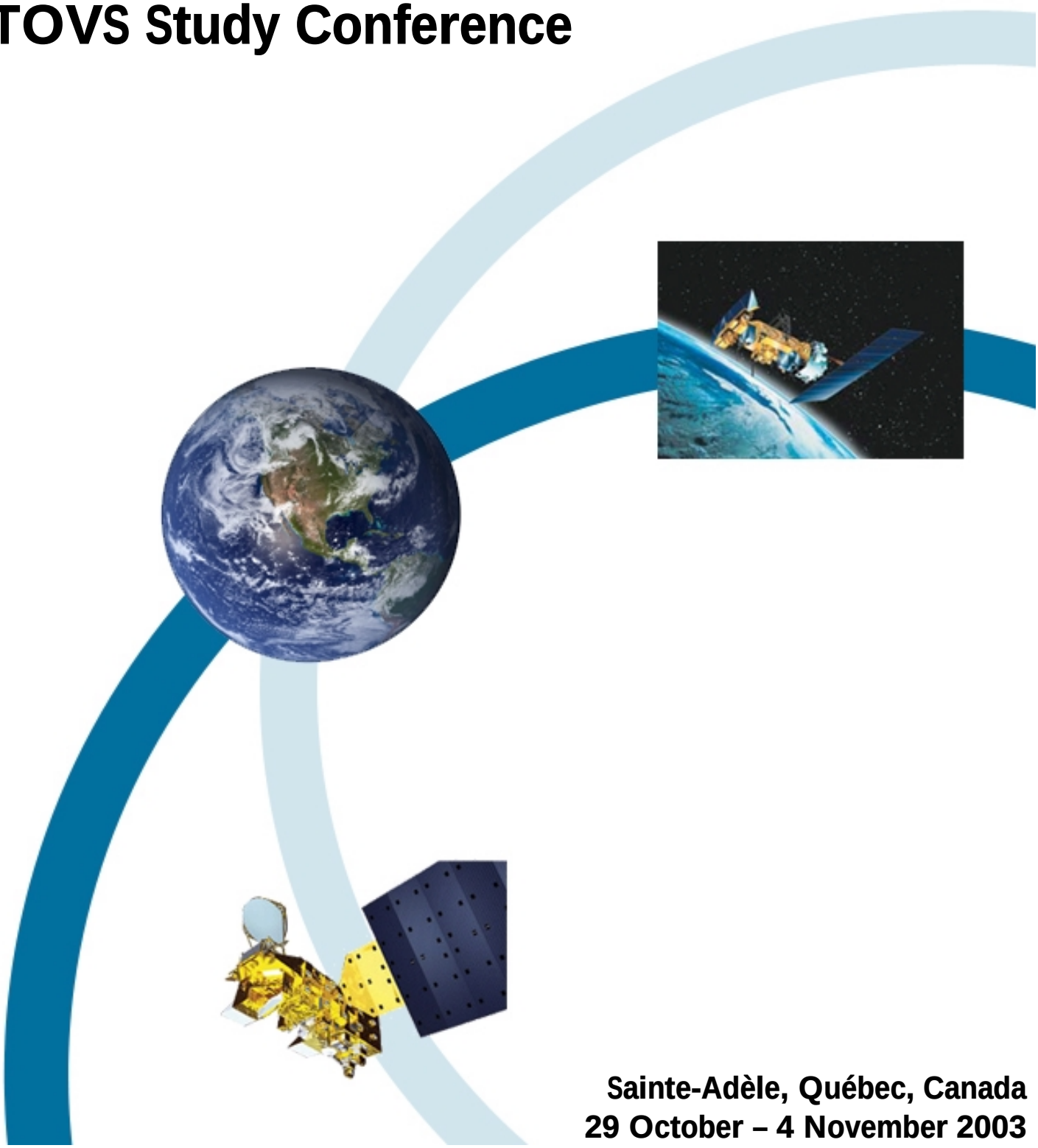

Sainte-Adèle, Québec, Canada
29 October – 4 November 2003